Optimal conditions for hemicelluloses extraction from Eucalyptus globules wood: hydrothermal treatment in a semi-continuous reactor

Gianluca Gallina [a], *Álvaro Cabeza* [a], *Pierdomenico Biasi* [b] *and Juan García-Serna* [a*]

[a] Department of Chemical Engineering and Environmental Technology, High Pressure Processes Group, University of Valladolid, Valladolid, ES-47011, Spain

[b] Process Chemistry Centre, Laboratory of Industrial Chemistry and Reaction Engineering, Åbo Akademi, Biskopsgatan 8, Turku/Åbo, FI-20500, Finland

**To whom correspondence should be addressed. E-mail:* jgserna@iq.uva.es (J. García-Serna)

Abstract

Optimal conditions for hemicellulose extraction from wooden biomass in a semi-continuous system have been assessed in this work. This study would constitute the first stage for a profitable and green industrial process. *Eucalyptus globulus* was selected as raw material due to its low water consumption, high growth and its efficiency in lignocellulose production. Moreover its cultivation is very popular in southern Europe. Samples of 5.0 g of wood were fractioned using a pressurized hot water semi-continuous system, to produce sugars (pentoses and hexoses) and a solid residue enriched in lignin.

Five flow rates between 2.50 and 20.00 mL/min and four temperatures between 135.0 and 285.0 ºC were tested in order to maximize the production of sugars, avoiding the formation of degradation products.

Optimum conditions for the extraction of hemicellulose were identified at 185.0 ºC and 5.00 mL/min, leading to a pentoses yield of 67.409 wt%, with 0.702 wt% of degradation products. Almost all the pulp is extracted at 285.0 ºC.

SEM images show very well the changes in the wood structure at different temperatures.

A kinetic model was developed, describing the extraction and hydrolysis of hemicellulose and cellulose with absolute average deviations around 10 % for sugar extracted mass.

Keywords

Eucalyptus, hemicelluloses, fractionation, biorefinery, semi-continuous.

1. Introduction

Cellulose and hemicellulose contained in woody biomass can be hydrolysed to monomeric sugars, which can be further fermented to ethanol, or can be converted in higher value products [1-3]. Xylose from hemicellulose, for instance, can be converted to furfural, which is a precursor used in different fields, such as oil refining, plastics, pharmaceutical, and agrochemical industries [4]. L-Xylose can be also hydrogenated or enzymatically transformed to xylitol, which is a sweetening agent and is also used for preventing tooth decay [5]. HMF (Hydroxymethylfurfural) derived from hexose sugars can be oxidized to obtain 2,5-furandicarboxylic acid, which can substitute terephthalic acid (PTA) in the production of polyesters and other current polymers containing an aromatic moiety [6]. The idea of transforming biomass to energy, materials, and chemicals, defines the concept of a biorefinery [7-10], particularly being an interesting topic nowadays, considering the issues related to fossil combustibles and derivatives.

Direct fermentation of biomass to ethanol by enzymatic digestion cannot succeed without a pre-treatment to modify the cross-linked structure between lignin and polysaccharides and reduce the biomass recalcitrance to enzymatic hydrolysis [11, 12] .

A promising, clean and cheap way to fractionate lignocellulosic materials is the so called autohydrolysis, which simply consists of treating biomass with hot pressurised liquid water: during the reaction, most of the hemicelluloses are extracted and hydrolysed to monomers, with a consequent release of acetic acid originated from the cleavage of the acetyl groups bonded to the oligosaccharides; a lower amount of cellulose is released, due to the crystalline structure of the polymer, which makes it more difficult to dissolve and hydrolyse [13]. Moreover, the structure of the cell walls becomes more accessible to enzymatic attacks. Hydrolysis and degradation of the extracted products will be more severe along with temperature, residence time and low pH.

In comparison with other pre-treatments with mineral acids [14, 15] or bases [16, 17] added to the reaction media, autohydrolisis has a lower environmental impact, as the only reagent is water and no further detoxification treatments are required to neutralize the sludges. Autohydrolysis is also a cost

effective process, as the variation of pH in the liquors is very low and there is no corrosion of the equipment [18, 19]. In literature there are several examples of this process, performed with different biomass crops and residues. Agriculture wastes like wheat straw [20, 21], corn stover [22, 23] and rice straw [24, 25] have been intensively explored for this kind of process, due to their abundance and easy availability. Also many woody biomass have been widely used [26-28], as they contain less inorganic substances than agricultural crops [29] and contain more acetyl groups that enhance the catalytic activity of the process (in particular hardwood species) [18].

A profitable biomass for hemicellulose extraction is needed. This raw material should have a high growth rate, a low water consumption and a high content of hemicellulose. *Eucalyptus globulus* has all these characteristics and, in particular, it is the world's most efficient tree for producing pulp. Moreover, eucalyptus wood has a high density enabling the tree to capture large amounts of CO_2 (0.1359 t CO_2 /year/tree) and thus to accumulate more carbon per unit of volume compared to other forest species [30]. A high biomass yield and a low water consumption (306 L/kg dry material against 400 L/kg dry material for oak trees or 1000 and 2000 L/kg dry material for herbaceous species like corn and soya respectively) [30] make eucalyptus very attractive from an industrial point of view, not only for paper production, but also as a sustainable and carbon-neutral source for liquid fuels and bio-compounds.

In addition, eucalyptus is a tree of considerable importance in the Iberian Peninsula and in the world, due to its wide expansion and its spread use in industrial applications, mainly for the paper industry.

Garrote et al. studied the fractionation of *Eucalyptus globulus* wood [31] , the extraction of hemicellulose and the production of xylose from xylooligosaccharides [32], after pre-treatments in a batch reactor.

While there are several studies dealing with the autohydrolysis in batch reactors [33-39], only a smaller number of articles regards flow-through reactors [11, 40, 41].

In our study, we investigate the autohydrolysis of *Eucalyptus globulus* wood in a semi-continuous reactor, consisting in a tubular reactor loaded with wood chips, constantly through by pressurized hot water. This kind of set-up allows a high solid / liquid ratio and a rapid removal of the products,

preventing their degradation. Moreover a continuous supply of fresh water to the system guarantees a high concentration gradient at the solid-liquid interface, thus, enhancing the mass transfer respect to a batch or a semi-batch reactor [29].

Recent studies have been completed using flow-through extractions with corn stover biomass. Authors found that flow-through extraction resulted in higher xylose yield, and greater lignin removal respect to batch reactors [42]. The removal of lignin makes the remaining cellulose after the pre-treatments more digestible by the enzymes [43].

Respect to continuous reactor, where biomass and water are continuously fed into the reactor, in semi-continuous reactor solid pumping and extreme milling is avoided, reducing considerably the costs.

All these characteristics make, in our view, the semi-continuous reactor the best for the pre-treatment of biomass in a future industrial scenery.

Different liquid flow rates (2.50, 5.00, 10.00, 15.00, 20.00 mL/min) and different reaction temperatures (135.0, 185.0, 235.0, 285.0 °C) were tested in order to maximize the yield of polysaccharides extraction avoiding the formation of degradation products that would inhibit a further fermentation step [44].

SEM pictures of the exhausted solid bed were taken to analyse the structure of the wood after the pre-treatments.

In addition to optimizing the temperature, whose effect was already explored in batch systems [28, 31], the liquid residence time for the extraction of hemicellulose from eucalyptus in a semi-continuous reactor was optimized in this work. Effects of the residence time were suddenly checked at temperature not normally suitable for the extraction of hemicellulose.

Moreover an auto catalytic kinetic model developed by our group, and previously validated for another raw material (holm oak), was simplified and implemented. It can be stated that even changing the biomass, the model represent very well the extraction and hydrolysis in a semi-continuous reactor.

2. Materials and Methods

2.1 Materials

Eucalyptus globulus wood used as the main raw material of all the experiments originated from Cantabria (Spain). Wooden branches were cut in slices with a jigsaw, and then reduced to small pellets with an average Feret diameter of 0.6 cm. The composition of the raw material (Table 1) in terms of structural carbohydrates, extractives, ashes, humidity and lignin were determined according to the standard methods published by National Renewable Energy Laboratory (NREL) [45].

The column used for the separation of the compounds was SUGAR SH-1011 Shodex at 50.0 ºC and a flow of 0.80 mL/min, using a solution of 0.01N of sulphuric acid and water Milli-Q as mobile phase. A Waters IR detector 2414 and Waters dual λ absorbance detector 2487 (210 nm and 254 nm) was used to identify the sugars and their derivatives.

The calibration reagents used for HPLC analysis were: cellobiose (+98%), glucose (+99%), fructose (+99%), glyceraldehyde (95%), pyruvaldehyde (40%), arabinose (+99%), glycolaldehyde (+98%), 5-hydroxymethylfurfural (99%), lactic acid (85%), formic acid (98%), acrylic acid (99%), mannose (+99%), xylose (+99%), galactose(+99%), levulinic acid (≥ 97%), furfural (+99%), acetic acid (+99%) purchased from Sigma and used without further modification.

For the analysis of sugars sulphuric acid (96%) and calcium carbonate (≥ 99.0%), purchased from Panreac were used.

2.2 Reactor set-up for the experiments

The experiments were carried out in a laboratory-scale fixed bed reactor (R-01, 38 cm length, ½" O.D. SS316 piping, 0.37" I.D.) (as depicted in Figure 1).

The reactor was charged with 5.00±0.01 g of wood pellets, two metallic filters were placed at the top and at the bottom, in order to avoid the loss of solid particles during the experiments. Deionized water was introduced continuously into the reactor, in up-flow, using a PU-2080 HPLC pump.

The feed flow, at room temperature, was preheated by the out-flow of the reactor, through a concentric tube heat exchanger working in counter current (E-02, 70 cm length, 1/4”-3/8”). A preheater (E-01, 200 cm of 1/8” AISI 316 piping) was placed after the heat exchanger and located, together with the reactor, inside a former chromatographic oven HP5680, which could be set at the desired temperature.

Pressure was controlled by a Go-backpressure valve (BPV-01) installed at the liquid outlet. The out-flow pH was measured online through an electronic pH-meter (Nahita model 903).

A heat exchanger allowed to recover between the 70% and 85% of the energy input; the plant, even if in laboratory scale, was designed to operate according to green concepts of energy saving.

2.3 Experimental procedure and analytical methods

A set of 9 experiments was carried out: 5 with changing water flow rate (2.50, 5.00, 10.00, 15.00, 20.00 mL/min), at constant temperature (185.0°C), and 4 with changing temperature (135.0, 185.0, 235.0, 285.0 °C) at constant flow rate (5.00 ml/min). Pressure was kept constant at 100.0 bar, in order to guarantee the liquid phase of the aqueous reaction media at all the operated temperatures. In the initial stage of the experiments the reactor was filled with a constant amount of wood, and then connected to the system. A cold liquid pressure test was made before each experiment, in order to check the presence of leaks in the system, and to ensure the complete wetting of the wood. Water was then heated in a pre-heating capillary and when the reaction temperature was reached the oven was turned on and the pump was set to the desired feed water flow. Time 0 was defined as the time in which the first drop of liquid left the system, at this point the measurement of pH started and a first sample of liquid was taken.

The total time of each experiment was 90 min, 20.0 mL liquid samples were taken every 10 min, pH was recorded online every 1 minute during the first 30 min, and then every 2 minutes until the end of the tests. After 90 min, the pump was switched off to zero flow and the oven temperature lowered to 20.0 ºC; the system was then slowly depressurised, the reactor untightened and all its content was collected in a beaker and dried for 24h at 60.0 °C. Finally the empty reactor was reconnected to the system and deionized water was flushed to clean all the pipes.

To determine the amount of sugars extracted and the degradation products produced after the autohydrolysis, a posthydrolysis process of the extracted liquor was performed to break all the oligomers in monomers, and allowing the accurate count of the extracted products after a HPLC separation.

10.0 mL of each sample were completely hydrolyzed with 4.0 mL of sulfuric acid 96 %wt. and consequently incubated in an oven for 30 min at 30.0 °C. The mixtures were then diluted with 86.0 mL of deionized water and warmed in an oven for 1 hour at 121.0 ºC. At the end of the acid hydrolysis, the samples were cooled down to room temperature, calcium carbonate was added in order to raise the pH to a value between 6 and 7, the solution was filtered through 0.22 μm nylon filters and the content of sugars was determined by HPLC.

The solid resulting from each experiment was processed as explained by the standard methods published by National Renewable Energy Laboratory (NREL) [45], residue of Klason lignin was determined as well as the amount and quality of soluble compounds not extracted by the thermohydrolysis.

Unprocessed eucalyptus wood was characterized as explained in paragraph 2.1, in order to relate the amount of compounds extracted during the experiments with the raw material composition.

Main peaks and areas were identified and calculated through a band-analysis via fast Fourier transform (FFT) and band-adjustment by Gaussian functions. The adjustment was done by minimizing the quadratic error using a Nelder-Mead algorithm.

2.4 Uncertainty analysis

In order to check the reliability of the experimental data, the uncertainty of all of them was calculated. Regarding the concentration obtained by HPLC Eq. 1 was used to consider the repeatability, the experimental data deviation and the effect of the calibration. Once this value was obtained, a typical propagation expression was used to obtain the uncertainty of the values calculated following the NREL standard methods [45].

$$s_{\mathrm{x}} = \frac{s_{\mathrm{y}}}{\mathrm{m}} \cdot \sqrt{\frac{1}{L} + \frac{1}{N} + \frac{(\overline{y_{\mathrm{x}}} - \overline{y})^2}{m^2 \cdot S_{\mathrm{xx}}}}$$

$$s_{\mathrm{y}} = \sqrt{\frac{\sum(y_{\mathrm{i}} - \hat{y}_{\mathrm{i}})^2}{N-2}} \qquad (1)$$

$$s_{\mathrm{xx}} = \sum_{i=1}^{\mathrm{N}} (x_{\mathrm{i}} - \overline{x})$$

3. Results and discussion

The total amount of sugars and acetyl groups contained in eucalyptus wood was equal to 64.532 wt% of the total mass (sum of glucans, xylan, arabinan abd acetyl groups represented in Table 1).

Semicontinuous extraction/reaction is particular in terms of residence time. In the semicontinuous plant two different reaction times were defined in the system:

- solid residence time τ_{sol}, which was constant for all the tests (always 90 min), and corresponded to the total duration time of the experiments, as the solid was static inside the reactor;
- liquid residence time τ_{liq}, which varied in relation with the operational conditions of the experiment, in particular with the liquid flow rate and with the porosity (void volume of the bed). An initial porosity ε_0 was defined, as the ratio between the volume of the empty spaces in the reactor at the beginning of the experiments, and the total volume of the empty reactor. ε_0 was determined in the lab to be 0.70. A final porosity ε_{f} was calculated (Eq. 2) taking into account the mass variation of the solid particles inside the reactor between the beginning and the end of each experiment; m_0 and m_{f} corresponded to the initial and the final mass of the solid in the reactor. Liquid residence time (Eq. 3) was calculated considering an average porosity $\varepsilon_{\mathrm{av}}$ between the initial ε_0 and the final porosity ε_{f} of the bed in each experiment. To calculate the final porosity, it was assumed that the density of the wood particles remained constant during time, and that there were only variations in the volume of the particles.

$$\varepsilon_f = \varepsilon_0 + (1 - \varepsilon_0)\frac{(m_0 - m_f)}{m_f} \quad (2)$$

$$\tau_{liq} = \frac{V}{\dot{V}}\varepsilon_{av} \quad (3)$$

The liquid residence time is influenced mostly by the liquid flow rate and slightly by the temperature (meanwhile we operated under liquid phase conditions, and the changes in liquid density with temperature are low). The most important variable is temperature, as an increase in temperature leads to a greater extraction of soluble compounds from the wood (as it will be shown), which means a decrease of the solid particles volumes along with an increase of the porosity of the bed. The density of the solution was considered to be equal to the density of water, as the concentration of soluble compounds was always low, and did not influence the residence time of liquid.

A summary of experimental conditions and results obtained is shown in Table 2. All the results were calculated as cumulative values at the end of each experiment. Figure 2 represent the cumulate values of sugars and acetic acid resulting from the experiment at 185 °C and 5 mL/min, where the mass of the compounds detected by HPLC are represented in function of the solid residence time. Final values of all experiments (calculated at τ_{sol} =90 min) are shown in Table 2.

At first glance, one can see how the major percentage of sugars obtained correspond to xylose, while glucose and arabinose were exceedingly lower. Acetic acid was also measured, which was the ultimately responsibly of the decrease in the pH during the experiments (see pH evolution in Figure 3).

"Yield tot" indicates the fraction of soluble compounds (sugars and degradation products) in the liquid respect to the total amount of soluble compounds in the raw material, detected by HPLC.

Mass balance was checked ($m_{balance}$) by summing up the amounts of soluble compounds in the extracted liquor and in the exhausted solid, detected by HPLC, and then dividing the result to the amount of soluble compound in the raw material. In all the cases the balance can be considered respected. The deviations from 100% may be due, in addition to the uncertainty explained in section 2.4, to possible peak integration errors. Some peaks are in fact slightly overlapping, and the calculation of their area may deviate slightly from the correct value.

The yields of hexoses (so-called C6) and pentoses (so-called C5) are calculated by dividing the mass of pentose and hexose sugars extracted, by the total amount of sugars in the raw material. Lignin percentage in the exhaust solid with respect to the initial weight of the raw material is represented in the last column of Table 2.

3.1. Effect of temperature

In figure 3a, the yield of soluble compounds is represented as a function of temperature, with a constant liquid flow rate of 5.00 mL/min. Degradation products, in the second vertical axe, are calculated as the sum of formic acid, furfural, HMF and pyruvaldehide. Acetic acid was not considered as a degradation product becouse it results from the deacetylation of hemicellulose.

At constant flow rate, the amount of solubilised compounds increased linearly with increasing the temperature.

At 135.0 °C, there is not extraction, while 185.0°C were enough to extract hemicellulose with a pentoses yield of 67.409 wt%; cellulose was not depolimerized at these conditions, and degradation products were below 1 wt% with respect to the original weight of the raw material.

At 235.0 °C, cellulose started to be depolymerized and the yield of hexoses increased to 12.436 wt%; pentoses yield decreased to 62.817 wt% while the amount of degradation products reached the 9.613 wt% of the original mass of wood.

Yield of hexoses became 64.703 wt% at 285.0 °C, as the increasing of temperature promoted the depolymerization of cellulose. At the same conditions, hemicellulose extraction reached its maximum point with a yield of 82.369 wt% for pentoses, while the total amount of degradation products only increased slightly with respect to the previous experiment. The sum of C5 sugars with acetic acid furfural and formic acid gives the amount of hemicellulose extracted, resulting in a yield of 91.01 wt%. Cellulose yield, calculated by summing C6 sugars with HMF and pyruvaldehyde, resulted to be 76.10 wt%.

At the beginning of the process, hemicellulose is more easily extracted than after few minutes, as it can be seen in the cumulated curve in Figure 2. Therefore, two kinds of hemicellulose can be distinguished in wooden biomass: one easier to extract, and the other closely associated with cellulose, which can be removed only with more severe conditions [46]. It looks like that at 285.0 °C, the structural modification of the cell walls and the removal of the cellulose, allowed the extraction of the associated hemicellulose. Extraction of cellulose starts at 235.0 °C with a yield of 12.436 wt% for C6, reaching a value of 64.703 wt% at 285.0 ºC. 85.684 wt% of the pulp is extracted at this temperature, leaving a residual solid containing mainly lignin, with a few fibres of cellulose and hemicellulose oligomers.

pH (figure 3b) reached a minimum value and then started to increase slowly: increasing the temperature, pH increased slower after the minimum point, and reached a lower value at the end of the experiment.

High temperatures indeed led to a stronger depolymerisation of hemicellulose, and thus to a greater deacetylation and further reduction to acetic acid. At 135.0 °C pH kept decreasing during the whole reaction, without reaching a minimum value, exhibiting the lowest deacetylation rate. The kinetic of depolymerisation of hemicellulose was very slow [47, 48], and the amount of acid produced was very low compared with the other experiments.

3.2. Effect of liquid residence time

Liquid residence time plays an important role in the autohydrolysis process, as it is directly related with the residence time of the main reagent (water) and the solubilised compounds inside the system. This drasticly determines the concentration of acetic acid in the liquor, and subsequently the free protons to induce a further hydrolysis.

The yield of pentoses was almost invariable at 185.0 °C under different liquid residence times (figure 3c), with the exception that it slightly decreased at τ_{liq} = 7.79 min. The yield of hexoses was very low in all experiments, as the operational temperature was not sufficiently high to target the cellulose activation energy and depolymerize it; glucose detected derived surely from the hemicellulose.

There was no decomposition of sugars when the liquid residence time was between 0 and 1.91 min, degradation products appeared at τ_{liq} = 3.84 min, at τ_{liq} = 7.79 min the amount of degradation products results to be 4.55 wt% with respect to the raw material mass.

It is well-known that under high temperatures the acetyl groups that bind hemicellulose with lignin are released and reduced to acetic acid [49], leading to the chain reaction called autohydrolysis of hemicellulose [32, 36].

A temperature of 185.0ºC and a flow rate of 5.00 mL/min lead to a yield of C5 sugars of 67.409 wt%, comparable to that obtained by Garrote et al. with *Eucalyptus globulus* wood, in a batch reactor at 181 ºC (58.4 wt%) [50]. Lower flow rates lead to the decomposition of sugars, while higher flow rates do not improve the extraction, but are not recommended as they would lead to greater difficulty in the separation.

In Figure 3d it can be seen that pH decreased rapidly, starting from a value around 5.5 (pH of deionised water) and reaching a minimum value around pH = 3.0 at about 20 minutes from the beginning of the reaction. After that time, it started to increase slowly, due to the reduction in acetyl groups in the hemicellulose along with time and the continuous incoming water. At constant temperature, with the lowest flow rate (2.50 mL/min) pH was almost constant after τ_{sol} = 20 min; with higher flow rates pH increased more rapidly, and with 20.00 mL/min the velocity of neutralization was the highest, and the highest final pH at τ_{sol} = 90 min is reached (pH = 4.10). The lowest pH value is reached with 2.50 mL/min (pH = 2.93) and the highest with 20.00 mL/min (pH = 3.20).

In accordance with other works [43, 51] it can be stated that powering the mass transfer trough the increase of the flow rate, leads to the higher removal of hemicellulose from the wood. Long liquid residence times enhance the hydrolysis of the oligomers, and thus the production of acetic acid that catalyses the depolymerisation of oligomeric xylanes and further the degradation of monomers in the liquid phase.

3.3. Kinetic model for biomass fractionation

A simplified kinetic model was proposed for the overall extracted biomass, considering the variation of temperature and flow rate in the process. This model was based on a preliminary model for holm oak hydrothermal fractionation, which was performed by our research group [52] and has been used here to help in the clarification of the main effects.

In the solid phase, polymers start to depolymerize into monomeric sugars. Therefore, cellulose is fractionated to hexose monomers and hemicellulose to mainly pentose monomers and acetic acid. In parallel, hemicellulose, cellulose and deacetylated hemicellulose are partially solubilized by water, where they also are converted into monomers. The latter, only would be soluble at temperatures greater than 235 ºC. Regarding cellulose, its degradation is only considered at temperatures above 235.0 °C. Finally, acetic acid dissociation in protons and aqueous anions was introduced by an equilibrium constant. Thus, the reaction pathway includes 6 reactions, 3 in solid phase and 3 in the liquid phase (see Figure 4).

The model was obtained applying a mass balance for each compound in both phases [52]. This mass balance includes the mass transfer between both phases, the kinetics of each compound and the effect of the extraction in the bed porosity by the factor φ . The final expressions for the mass balance in liquid phase and in solid phase are Eq. (4) and Eq. (5), respectively.

$$\frac{d(1-\varepsilon)\cdot C_{S_j}}{dt} = r_j - k_j \cdot a \cdot (C_{L_j}^{*} - \bar{C}_{L_j}) \qquad (4)$$

$$\frac{\delta C_{L_j}}{\delta t} = \frac{1}{\varepsilon}\cdot\left[r_j - \frac{u}{L}\cdot\frac{\delta C_{L_j}}{\delta z} - \varphi\cdot C_{L_j}\cdot\frac{dC_t}{dt} + k_j\cdot a\cdot(C_{L_j}^{*} - \bar{C}_{L_j})\right] \qquad (5)$$

Equilibrium concentration in liquid phase (C_{Lj}*) was obtained by the product of the concentration in the solid and an equilibrium constant (H_j), which represents the solubility of biomass (C_{Lj}*=H_j·C_{sj}).

Finally, kinetics (Eq. (6)) of each compound were calculated by an autocatalytic expression because it is useful to reproduce big changes in concentration. In liquid phase, they were multiplied by the proton concentration to include the auto-hydrolysis effect.

$$r_j = \sum_{i=1}^{i=n_{reac}} \Phi_{i,j} \cdot r_i$$

$$r_i = k_i \cdot \prod_{j=1}^{j=N} C_{f_j} \cdot \left(1 - \alpha_{i,j} \cdot \frac{C_{f_j}}{C_{f_t}}\right)^{\beta_{i,j}} \qquad (6)$$

Where α is the initial velocity factor and β the acceleration factor. The former is related with the resistance of the material against thermal degradation and its recommended value is 0.99 [53]. The latter represents how fast the degradation is once it has started.

3.3.1. Fit to experimental data

The developed model was used to adjust the experimental data of the extracted sugars, pentoses and hexoses and the pH evolution with time. In order to simplify the problem at high temperatures (greater than 185.0 ºC), the total amount of degradation products was assumed as sugars. Therefore, xylose, arabinose, furfural and formic acid were summed to calculate pentoses (C5); while, glucose, HMF and pyruvaldehyde to calculate hexoses (C6). The data obtained at 135.0 ºC were not used due to the low amount of biomass extracted at this operational condition. These fittings imply an optimization problem which was solved by the Broyden–Fletcher–Goldfarb–Shanno's method [54] . The objective function was the addition of the Average Absolute Deviation (A.A.D., see Eq. (7)) of these three profiles. The calculated parameters are arrayed in Table 4.

$$A.A.D. = \sum_{i=1}^{n} \frac{1}{n} \cdot \left|\frac{X_{exp} - X_{sim}}{X_{exp}}\right| \cdot 100 \qquad (7)$$

For the experiment at 285.0 ºC and 5.00 ml/min, the result of the adjustment is shown in Figure 5. The model was able to reproduce the evolution of pentose sugars and the pH, including the fact that the maximum in sugar concentration and the pH minimum took place at the same time. This agreement

shows that the model was able to successfully simulate the hemicellulose deacetylation. In addition, from the adjustment shown in Figure 5c, it can be concluded that the model also could reproduce the behavior of the hexose sugars, whose maximum delated around 60 min with respect to pentoses due to the high resistance of cellulose against hydrothermal degradation. Therefore, pentoses are extracted at the beginning of the operation and hexoses only are recovered at the final stage. However, around 20 % of sugar degradation was found at these operational conditions (Table 2), which is relatively high.

On the other hand, the A.A.D. for each experiment is arrayed in Table 3, being the average deviation 28.57, 39.20 and 5.7 % for pentoses, hexoses and pH respectively. These discrepancies were relative low taken into account the small amount of sample introduced in the reactor, the dilution of the samples, the complexity of the process (which has been simulated only with 8 compounds) and the biodiversity of the wood. In addition, the deviations fall up to 10.49 % and 13.17 % for C5 and C6, respectively, when the simulated and the experimental extracted mass are compared (Figure 2d and 2e). Therefore, it seems that the proposed model was able to reproduce the biomass fractionation by hydrothermal treatments.

3.3.2. Analysis of the model parameters

The physical sense of the parameters listed in the Table 4 was checked in this section. Regarding the mass transfer coefficient ($k_j \cdot a$), it was seen that all of them followed a linear function with flow (regression coefficients greater than 0.91) as it was expected. In the same way, it was calculated that the equilibrium constant or solubility (H_j) was enhanced with temperature linearly (R^2 greater than 0.91), which is a common behaviour in a solid dissolution process. Finally, it was also obtained that the kinetic constants (k_i) followed the Arrhenius' law with R^2 bigger than 0.97.

Furthermore, β increases with temperature and decreases with flow. Temperature is the main variable in this process and it enhances the extraction and justifying the increment in the acceleration factor (β). In contrast, the flow reduces the acceleration factor, although it also enhances extraction. The reason could

be that it also affects the residence time of the liquid phase, so a higher flow means less degradation product formation, more dilution and smother liquid profiles. It is also remarkable that the kinetics for cellulose fractionation are always lower than the kinetics for hemicellulose degradation, which agrees with the fact that cellulose is stronger than hemicellulose against hydrothermal degradation.

3.4. Lignin removal and structural alteration

Table 2 shows that at 185.0 °C lignin content in the exhaust solid is almost equal to the one in the raw material. At 235.0 °C and 5.00 mL/min a lignin reduction of approximately 15.00 wt% occurred, while a reduction of approx. 52 wt% at 285.0 °C occurred. A loss in lignin content in wooden biomass during hydrothermal pre-treatments is widely documented [12, 55], Leschinsky et al. reported that C thermal pretreatment of *Eucalyptus globulus* wood at 170 °C causes a loss of the molecular weight in lignin [56].

When lignocellulosic biomass is subjected to high temperature or mild acidic pre-treatments, lignin and lignin-carbohydrate complexes coalesce creating some spherical formations that migrate out to the wall cells and deposit in the surface of the residual biomass. These droplets have a negative effect on enzymatic hydrolysis of cellulose, affecting the efficiency of enzymatic conversion in a lignocellulosic biorefinery [57].

Figure 6 shows 3 SEM images of the Eucalyptus wood after treatment at 185.0 °C, 235.0 °C and 285.0 °C, with a liquid flow rate of 5.00 mL/min. At 185.0°C no evident changes are visible in the wood structure: the three-dimensional structure of lignin associated with linear molecules of cellulose is visible in figure 6a.

A modification in the structure of the wood is evident at 235.0 °C: lignin-carbohydrate droplets start to appear on the wood surface, as shown in figure 6b. The number of droplets increases significantly at 285.0 °C (figure 3c) where only sporadic fibres of broken cellulose are visible, directly connected through hemicellulose units (associated hemicellulose) as described in chapter 3.1.

While in batch reactors, all the droplets deposit on the surface and harden after the cooling, creating a barrier for enzymatic attach, in semi-continuous reactor this issue is lightened, as the liquid flow carries them constantly out of the system; this is evident from the lignin loss observed at high temperatures. This is another big advantage of using a semicontinuous reactor for the pretreatment of biomass.

4. Conclusions

In this study, we have focused in the effect of liquid flow rate on the extraction of hemicellulose from eucalyptus biomass, more specifically in the residence time. Operating in semi-continuous mode has the advantage of separating the residence time of the solid (easy to charge and keep inside a tubular reactor) and the liquid (moving through the bed created). Solid residence times between 20 and 40 min are perfect for extracting hemicelluloses, liquid residence times below 2.00 min avoid by-products with a temperature of 185° C. The influence of the flow is not perceived at 135 ºC, while at higher temperatures, the increase in yield is counterbalanced by the formation of degradation products. A simplified model considering an auto catalytic kinetics represents the operation very well. This work establishes the basis of the scale-up of the semi-continuous hydrothermal reaction.

Acknowledgements

The authors acknowledge the Spanish Economy and Competitiveness Ministry, Project FracBioFuel: ENE2012-33613 and the regional government (Junta de Castilla y León), Project Reference: VA330U13 for funding. MEng. Gianluca Gallina wish to acknowledge the Spanish Economy and Competitiveness Ministry for the scholarship/predoctoral contract BES-2013-063556. Alvaro Cabeza also wish to acknowledge the Spanish Economy and Competitiveness Ministry for the scholarship/predoctoral contract FPU2013/01516.

Abbreviations and symbols

Greek letters

$\alpha_{i,j}$: Initial velocity factor for the compound "j" in the reaction "i", dimensionless.

$\beta_{i,j}$: Acceleration factor for the compound "j" in the reaction "i", dimensionless.

β_C: Acceleration factor for cellulose, dimensionless.

β_{Hc}: Acceleration factor for hemicellulose, dimensionless.

$\mathcal{E}$: Porosity of the bed, dimensionless.

$\mathcal{E}_f$: Porosity of the bed, calculated at the end of the experiment, dimensionless.

$\mathcal{E}_{av}$: Average porosity of the bed, between the beginning and the end of the experiment, dimensionless.

$\mathcal{E}_0$: Porosity of the bed, calculated at the end of the experiment, dimensionless.

φ: Relation factor between porosity and the total concentration in solid phase, dimensionless.

$\Phi_{i,j}$: Stoichiometric coefficient of the compound "j" for the reaction "i", mg.

τ_{sol} : residence time of solid inside the reactor, min

τ_{liq} : residence time of liquid inside the reactor, min

Symbols

C_{f_j}: Concentration of the compound "j" in the phase "f", mg/L

C_{L_j}: Concentration of the compound "j" in the liquid phase, mg/L

$\bar{C}_{L_j}$: Average concentration of the compound "j" along the reactor in liquid phase, mg/L

$C_{L_j}^*$: Equilibrium concentration of the compound "j" in liquid phase, mg/L

C_{S_j}: Cocnetration of the compound "j" in the solid phase, mg/L

C_t: Total concentration in the solid, mg/L

Q: Liquid flow rate, mL/min

Ea/R: Activation energy, K

H_j: Equilibrium constant between the solid and the liquid, dimensionless

k: Pre-exponential factor of the kinetic constant, $mg^{-1} \cdot min^{-1}$

k_i: Kinetic constant, $mg^{-1} \cdot min^{-1}$

$k_j \cdot a$: Mass transfer coefficient multiplied by the specific exchange area, min^{-1}

N: Number of compounds, dimensionless

n_{rec}: Number of reactions, dimensionless

L: Length of the reactor, m

t: Operating time, min

r_i: Reaction velocity "i", mg/min·L

r_j: Reaction rate of the compound "j", mg/min·L

R^2: Coefficient R^2, dimensionless

T: Operating temperature, ºC

u: Liquid velocity in the reactor, m/min

$x_{i_{EXP}}$: Experimental value of the fitted variable

$x_{i_{SIM}}$: Simulated value of the fitted variable

z: Coordinate along the length of the reactor, dimensionless

s_x: uncertainty of the experimental concentration, ppm

s_y: standard deviation of the calibration patrons, ppm

s_{xx}: deviation of the HPLC areas, dimensionless

L: number of experiment repetitions, dimensionless

N: number of calibration points, dimensionless

m: slope of the calibration, ppm

x_i: experimental HPLC area, dimensionless

$\overline{x}$: average experimental HPLC area, dimensionless

y_i: patron concentration "i", ppm

$\widehat{y_i}$: calculated patron concentration "i", ppm

$\overline{y_x}$: average experimental concentration, ppm

$\overline{y}$: average patron concentration, ppm

References

[1] F. Cherubini, The biorefinery concept: Using biomass instead of oil for producing energy and chemicals, Energy Conversion and Management, 51 (2010) 1412-1421.
[2] I. Egües, M.G. Alriols, Z. Herseczki, G. Marton, J. Labidi, Hemicelluloses obtaining from rapeseed cake residue generated in the biodiesel production process, Journal of Industrial and Engineering Chemistry, 16 (2010) 293-298.

[3] S.-H. Yoon, A. van Heiningen, Green liquor extraction of hemicelluloses from southern pine in an Integrated Forest Biorefinery, Journal of Industrial and Engineering Chemistry, 16 (2010) 74-80.
[4] C. Rong, X. Ding, Y. Zhu, Y. Li, L. Wang, Y. Qu, X. Ma, Z. Wang, Production of furfural from xylose at atmospheric pressure by dilute sulfuric acid and inorganic salts, Carbohydr Res, 350 (2012) 77-80.
[5] P. Mäki-Arvela, B. Holmbom, T. Salmi, D.Y. Murzin, Recent Progress in Synthesis of Fine and Specialty Chemicals from Wood and Other Biomass by Heterogeneous Catalytic Processes, Catalysis Reviews: Science and Engineering, 49 (2007) 197 - 340.
[6] P.N.N.L. (PNNL), N.R.E.L. (NREL), Top Value Added Chemicals From Biomass in: U.S.D.o. Energy (Ed.), 2004.
[7] J.H. Clark, V. Budarin, F.E.I. Deswarte, J.J.E. Hardy, F.M. Kerton, A.J. Hunt, R. Luque, D.J. Macquarrie, K. Milkowski, A. Rodriguez, O. Samuel, S.J. Tavener, R.J. White, A.J. Wilson, Green chemistry and the biorefinery: A partnership for a sustainable future, Green Chemistry, 8 (2006) 853-860.
[8] M. González, A. García, A. Toledano, R. Llano-Ponte, M.A. De Andrés, J. Labidi, Lignocellulosic feedstock biorefinery processes. Analysis and design, Chemical Engineering Transactions, 17 (2009) 1107-1112.
[9] D. Murzin, Chemical Engineering for Renewables Conversion, First ed., 2013.
[10] J.J. Bozell, G.R. Petersen, Technology development for the production of biobased products from biorefinery carbohydrates-the US Department of Energy's "Top 10" revisited, Green Chemistry, 12 (2010) 539-554.
[11] T. Rogalinski, T. Ingram, G. Brunner, Hydrolysis of lignocellulosic biomass in water under elevated temperatures and pressures, The Journal of Supercritical Fluids, 47 (2008) 54-63.
[12] Y. Pu, F. Hu, F. Huang, B. Davison, A. Ragauskas, Assessing the molecular structure basis for biomass recalcitrance during dilute acid and hydrothermal pretreatments, Biotechnology for Biofuels, 6 (2013).
[13] P. Mäki-Arvela, T. Salmi, B. Holmbom, S. Willför, D.Y. Murzin, Synthesis of sugars by hydrolysis of hemicelluloses- A review, Chemical Reviews, 111 (2011) 5638-5666.
[14] F. Carrasco, C. Roy, Kinetic study of dilute-acid prehydrolysis of xylan-containing biomass, Wood Science and Technology, 26 189-208.
[15] J. Arreola-Vargas, V. Ojeda-Castillo, R. Snell-Castro, R.I. Corona-González, F. Alatriste-Mondragón, H.O. Méndez-Acosta, Methane production from acid hydrolysates of Agave tequilana bagasse: Evaluation of hydrolysis conditions and methane yield, Bioresource Technology, 181 (2015) 191-199.
[16] S.M. Hosseini, H.A. Aziz, Syafalni, M.V. Kiamahalleh, Evaluation of significant parameters on alkaline pretreatment process of rice straw, KSCE Journal of Civil Engineering, 17 (2013) 921-928.
[17] Y. He, Y. Pang, X. Li, Y. Liu, R. Li, M. Zheng, Investigation on the Changes of Main Compositions and Extractives of Rice Straw Pretreated with Sodium Hydroxide for Biogas Production, Energy & Fuels, 23 (2009) 2220-2224.
[18] G. Garrote, H. Domínguez, C.J. Parajó, Hydrothermal processing of lignocellulosic materials, Holz als Roh- und Werkstoff, 57 191-202.
[19] H. Amiri, K. Karimi, Autohydrolysis: A promising pretreatment for the improvement of acetone, butanol, and ethanol production from woody materials, Chemical Engineering Science, 137 (2015) 722-729.
[20] F. Carvalheiro, T. Silva-Fernandes, L.C. Duarte, F.M. Gírio, Wheat straw autohydrolysis: Process optimization and products characterization, Applied Biochemistry and Biotechnology, 153 (2009) 84-93.
[21] D. Nabarlatz, A. Ebringerová, D. Montané, Autohydrolysis of agricultural by-products for the production of xylo-oligosaccharides, Carbohydrate Polymers, 69 (2007) 20-28.
[22] K.L. Kadam, C.Y. Chin, L.W. Brown, Optimization of a biomass fractionation process and evaluation of its economic feasibility, in: 2007 AIChE Annual Meeting, 2007.

[23] C.T. Buruiana, C. Vizireanu, G. Garrote, J.C. Parajó, Optimization of corn stover biorefinery for coproduction of oligomers and second generation bioethanol using non-isothermal autohydrolysis, Industrial Crops and Products, 54 (2014) 32-39.
[24] S. Imman, J. Arnthong, V. Burapatana, N. Laosiripojana, V. Champreda, Autohydrolysis of tropical agricultural residues by compressed liquid hot water pretreatment, Applied Biochemistry and Biotechnology, 170 (2013) 1982-1995.
[25] P. Moniz, J. Lino, L.C. Duarte, L.B. Roseiro, C.G. Boeriu, H. Pereira, F. Carvalheiro, Fractionation of hemicelluloses and lignin from rice straw by combining autohydrolysis and optimised mild organosolv delignification, BioResources, 10 (2015) 2626-2641.
[26] L. Senila, M. Senila, C. Varaticeanu, C. Roman, L. Silaghi-Dumitrescu, Autohydrolysis Pretreatment and Delignification of Silver Fir Wood to Obtain Fermentable Sugars for Bioethanol Production, Energy Sources, Part A: Recovery, Utilization and Environmental Effects, 37 (2015) 1890-1895.
[27] Z.M. Zhao, H.Q. Shi, G. Liu, N. Li, J. Zhang, M.H. Niu, Q.W. Ping, Dissolution and depolymerization of hemicelluloses of acacia wood during autohydrolysis, Zhongguo Zaozhi Xuebao/Transactions of China Pulp and Paper, 30 (2015) 6-11.
[28] T. Silva-Fernandes, L.C. Duarte, F. Carvalheiro, M.C. Loureiro-Dias, C. Fonseca, F. Gírio, Hydrothermal pretreatment of several lignocellulosic mixtures containing wheat straw and two hardwood residues available in Southern Europe, Bioresource Technology, 183 (2015) 213-220.
[29] P. Kilpeläinen, V. Kitunen, J. Hemming, A. Pranovich, H. Ilvesniemi, S. Willför, Pressurized hot water flow-through extraction of birch sawdust – Effects of sawdust density and sawdust size, Nordic Pulp & Paper Research Journal, 29 (2014) 547-556.
[30] ENCE, Sustainable forest management and Eucalyptus, in: ENCE Catalog 2009, 2009.
[31] A. Romaní, G. Garrote, F. López, J.C. Parajó, Eucalyptus globulus wood fractionation by autohydrolysis and organosolv delignification, Bioresource Technology, 102 (2011) 5896-5904.
[32] G. Garrote, H. Domínguez, J.C. Parajó, Generation of xylose solutions from Eucalyptus globulus wood by autohydrolysis–posthydrolysis processes: posthydrolysis kinetics, Bioresource Technology, 79 (2001) 155-164.
[33] Q. Hou, Y. Wang, W. Liu, L. Liu, N. Xu, Y. Li, An application study of autohydrolysis pretreatment prior to poplar chemi-thermomechanical pulping, Bioresour Technol, 169 (2014) 155-161.
[34] G. Garrote, H. Domínguez, J.C. Parajó, Kinetic modelling of corncob autohydrolysis, Process Biochemistry, 36 (2001) 571-578.
[35] D. Sidiras, F. Batzias, R. Ranjan, M. Tsapatsis, Simulation and optimization of batch autohydrolysis of wheat straw to monosaccharides and oligosaccharides, Bioresource Technology, 102 (2011) 10486-10492.
[36] T. Ojumu, B.a. AttahDaniel, E. Betiku, B. Solomon, Auto-hydrolysis of lignocellulosics under extremely low sulphuric acid and high temperature conditions in batch reactor, Biotechnology and Bioprocess Engineering, 8 (2003) 291-293.
[37] M.H. Sipponen, V. Pihlajaniemi, S. Sipponen, O. Pastinen, S. Laakso, Autohydrolysis and aqueous ammonia extraction of wheat straw: effect of treatment severity on yield and structure of hemicellulose and lignin, RSC Advances, 4 (2014) 23177-23184.
[38] J.V. Rissanen, H. Grénman, S. Willför, D.Y. Murzin, T. Salmi, Spruce Hemicellulose for Chemicals Using Aqueous Extraction: Kinetics, Mass Transfer, and Modeling, Industrial & Engineering Chemistry Research, 53 (2014) 6341-6350.
[39] L. Cheng, X.P. Ye, R. He, S. Liu, Investigation of rapid conversion of switchgrass in subcritical water, Fuel Processing Technology, 90 (2009) 301-311.
[40] X. Chen, M. Lawoko, A.V. Heiningen, Kinetics and mechanism of autohydrolysis of hardwoods, Bioresource Technology, 101 (2010) 7812-7819.
[41] T. Ingram, T. Rogalinski, V. Bockemühl, G. Antranikian, G. Brunner, Semi-continuous liquid hot water pretreatment of rye straw, The Journal of Supercritical Fluids, 48 (2009) 238-246.

[42] C. Liu, C.E. Wyman, Impact of Fluid Velocity on Hot Water Only Pretreatment of Corn Stover in a Flowthrough Reactor, in: M. Finkelstein, J.D. McMillan, B.H. Davison, B. Evans (Eds.) Proceedings of the Twenty-Fifth Symposium on Biotechnology for Fuels and Chemicals Held May 4–7, 2003, in Breckenridge, CO, Humana Press, Totowa, NJ, 2004, pp. 977-987.
[43] H. Pei, L. Liu, X. Zhang, J. Sun, Flow-through pretreatment with strongly acidic electrolyzed water for hemicellulose removal and enzymatic hydrolysis of corn stover, Bioresource Technology, 110 (2012) 292-296.
[44] M.S. Moreno, F.E. Andersen, M.S. Díaz, Dynamic Modeling and Parameter Estimation for Unit Operations in Lignocellulosic Bioethanol Production, Industrial & Engineering Chemistry Research, 52 (2013) 4146-4160.
[45] N.R.E. Laboratory, Determination of Structural Carbohydrates and Lignin in Biomass, in, Golden, CO, 2011.
[46] C.E. Wyman, S.R. Decker, M.E. Himmel, J.W. Brady, C.E. Skopec, L. Viikari, Hydrolysis of cellulose and hemicellulose, in: S. Dumitriu (Ed.) Polysaccharides: Structural Diversity and Functional Versatility, CRC Press, 2005, pp. 1023-1062.
[47] G.-J. Lv, S.-B. Wu, R. Lou, KINETIC STUDY FOR THE THERMAL DECOMPOSITION OF HEMICELLULOSE ISOLATED FROM CORN STALK, 2010.
[48] X.F. Sun, F. Xu, R.C. Sun, Z.C. Geng, P. Fowler, M.S. Baird, Characteristics of degraded hemicellulosic polymers obtained from steam exploded wheat straw, Carbohydrate Polymers, 60 (2005) 15-26.
[49] G. Garrote, H. Domínguez, J.C. Parajó, Study on the deacetylation of hemicelluloses during the hydrothermal processing of Eucalyptus wood, Holz als Roh- und Werkstoff, 59 (2001) 53-59.
[50] G. Garrote, M.E. Eugenio, M.J. Diaz, J. Ariza, F. López, Hydrothermal and pulp processing of Eucalyptus, Bioresource Technology, 88 (2003) 61-68.
[51] C. Liu, C. Wyman, The effect of flow rate of compressed hot water on xylan, lignin, and total mass removal from corn stover, Ind Eng Chem Res, 42 (2003) 5409 - 5416.
[52] A. Cabeza, F. Sobrón, F.M. Yedro, J. García-Serna, Two-phase modelling and simulation of the hydrothermal fractionation of holm oak in a packed bed reactor with hot pressurized water, Chemical Engineering Science, 138 (2015) 59-70.
[53] R. Capart, L. Khezami, A.K. Burnham, Assessment of various kinetic models for the pyrolysis of a microgranular cellulose, Thermochimica Acta, 417 (2004) 79-89.
[54] W. Press, S. Teukolsky, W. Vetterling, B. Flannery, Numerical recipes 3rd edition: The art of scientific computing, (2007).
[55] H. Trajano, N. Engle, M. Foston, A. Ragauskas, T. Tschaplinski, C. Wyman, The fate of lignin during hydrothermal pretreatment, Biotechnology for Biofuels, 6 (2013) 110.
[56] M. Leschinsky, G. Zuckerstätter, K. Weber Hedda, R. Patt, H. Sixta, Effect of autohydrolysis of Eucalyptus globulus wood on lignin structure. Part 1: Comparison of different lignin fractions formed during water prehydrolysis, in: Holzforschung, 2008, pp. 645.
[57] J.D. DeMartini, S. Pattathil, U. Avci, K. Szekalski, K. Mazumder, M.G. Hahn, C.E. Wyman, Application of monoclonal antibodies to investigate plant cell wall deconstruction for biofuels production, Energy & Environmental Science, 4 (2011) 4332-4339.

Table and Figure Captions

Table 1. Composition of the raw material

Table 2. Experimental table for the study of eucalyptus wood autohydrolysis in a semicontinuous reactor.

Table 3. A.A.D. of the fitted experiments.

Table 4. Mass transfer and kinetic parameters obtained from the fitting of the model to experimental data.

Figure 1. Schematic flow diagram of the experimental system. equipment: D-01 feeder, P-01 pump, E-01 feed water preheater, R-01 hydrothermal reactor, F-01 reactor air convection oven, E-02 preheat capillary, BPV-01 product depressurization Go-backpressure valve, E-03 product cooler, D-02 liquid product vessel.

Figure 2. Fraction of soluble compounds in liquid as a function of solid residence time at a constant liquid flow rate 5 mL/min and constant temperature 185.0 ºC.

Figure 3. Yield of soluble compounds as a function of temperature at a constant liquid flow rate 5 mL/min (a). pH in function of τ_{sol} at different temperatures and constant flow rate 5 mL/min (b). Yield of soluble compounds as a function of the liquid reaction time at 185.0°C (c). pH in function of τ_{sol} at different liquid flow rates and constant temperature 185.0°C (d).

Figure 4. Simplified reaction pathway for eucalyptus hydrothermal fractionation.

Figure 5. Adjustment of the experiment at 285.0 ºC and 5 ml/min. (a) Sugar C5, (b) pH and (c) Sugar C6 and comparison between the experimental and simulated extracted mass of C5 (d) and C6 (e) . C5-

SIM: Simulated concentration of sugars C5. C6-SIM: Simulated concentration of sugars C6. pH-SIM: Simulated pH. C5-EXP: Experimental concentration of sugars C5. C6-EXP: Experimental concentration of sugars C6. pH-EXP: Experimental pH.

Figure 6. SEM images of Eucalyptus exhausted wood after pretreatment at a) 185.0°C, b) 235.0 °C, and c) 285.0 °C with a liquid flow rate of 5 mL/min.

Tables and figures

Table 1.

wt%	wt%	wt%	wt%	wt%	wt%	wt%	wt%
Umidity	**Extractives**	**Ashes**	**Klason Lignin**	**Glucans**	**Xylan**	**Arabinian**	**Acetil Groups**
6.501	3.088	0.138	25.741	39.742	18.796	2.593	3.401

Table 2.

°C	mL/min	min	wt% [a]	wt% [a]	wt% [a]	wt% [a]
T	**Flow**	**t liq**	**Yield tot**	**Mass Balance**	**Yield C6**	**Yield C5**
185.0±1.1	2.500±0.010	7.65±0.15	26.042±0.067	102.014±0.214	0.419±0.002	51.417±0.050
185.0±1.1	5.000±0.010	3.82±0.11	26.237±0.052	100.231±0.205	2.282±0.005	67.409±0.031
185.0±1.1	10.000±0.010	1.90±0.10	21.695±0.039	100.453±0.202	0.731±0.002	60.476±0.019
185.0±1.1	15.000±0.010	1.27±0.10	22.931±0.039	100.636±0.202	0.000±0.012	67.486±0.008
185.0±1.1	20.000±0.010	0.95±0.10	22.043±0.037	98.741±0.196	0.000±0.010	65.847±0.010
135.0±1.1	5.000±0.010	3.69±0.11	0.313±0.000	98.857±0.221	0.000±0.000	0.985±0.000
185.0±1.1	5.000±0.010	3.82±0.11	26.237±0.052	100.231±0.205	2.282±0.005	67.409±0.031
235.0±1.1	5.000±0.010	3.92±0.11	45.476±0.083	98.039±0.189	12.436±0.022	62.817±0.037
285.0±1.1	5.000±0.010	4.12±0.11	85.684±0.153	102.629±0.177	64.703±0.114	82.369±0.050

wt% [b]	wt% [b]	wt% [b]	wt% [b]	wt% [b]	wt% [b]	wt% [b]	wt% [b]	wt% [b]
$w_{glucose}$	w_{xylose}	$w_{acetic\ acid}$	$w_{arabinose}$	$w_{formic\ acid}$	$w_{pyruvaldehyde}$	w_{HMF}	$w_{furfural}$	$w_{lignin\ residual}$
0.167±0.002	9.336±0.040	1.874±0.010	1.092±0.030	0.524±0.005	0.000±0.000	0.570±0.003	0.524±0.005	26.122±0.434
0.911±0.003	12.138±0.030	1.460±0.006	1.533±0.005	0.000±0.004	0.000±0.000	0.011±0.001	0.000±0.004	27.168±0.456
0.292±0.001	11.994±0.017	1.291±0.005	0.271±0.007	0.000±0.000	0.000±0.000	0.000±0.000	0.000±0.000	27.155±0.443
0.000±0.012	12.503±0.004	0.946±0.000	1.184±0.007	0.000±0.000	0.000±0.000	0.000±0.000	0.000±0.000	26.670±0.448
0.000±0.010	13.095±0.004	0.713±0.000	0.260±0.010	0.000±0.000	0.000±0.000	0.000±0.000	0.000±0.000	26.968±0.442
0.000±0.000	0.200±0.000	0.000±0.000	0.000±0.000	0.000±0.000	0.000±0.000	0.000±0.000	0.000±0.000	25.471±0.448
0.911±0.003	12.138±0.030	1.460±0.006	1.533±0.005	0.000±0.004	0.000±0.000	0.011±0.001	0.000±0.004	27.168±0.456
4.965±0.009	11.318±0.032	1.706±0.006	1.422±0.018	0.537±0.003	0.940±0.010	1.228±0.002	0.537±0.003	21.874±0.447
25.831±0.049	14.245±0.044	2.336±0.009	2.461±0.025	1.161±0.003	1.800±0.010	2.691±0.005	1.161±0.003	12.421±0.679

[a] Percentage of the components in the liquid respect to the weight of the component in the raw material.

[b] Percentage with respect to the total initial weight of the raw material.

Table 3.

T	Q	A.A.D. (%)[1]		
ºC	mL/min	C5	C6	pH
185	2.5	24.51	*	2.9
185	5	28.91	*	4.23
185	10	35.8	*	1.09
185	15	42.96	*	12.72
185	20	12.92	*	8.43
235	5	36.43	48.58	6.75
285	5	18.46	29.83	2.91
AVERAGE		28.57	39.20	5.57

T	Q	A.A.D. (%)[2]	
ºC	mL/min	C5	C6
185	2.5	15.80	*
185	5	9.38	*
185	10	7.03	*
185	15	8.22	*
185	20	8.67	*
235	5	8.08	14.37
285	5	16.27	11.97
AVERAGE		10.49	13.17

*Due to the low temperature, cellulose fractionation was assumed as negligible.[1] Deviation for the instant concentration. [2] Deviation for the extracted mass.

Table 4.

FLOW EFFECT								
Flow	k·a(min^{-1})						β_{HC}	β_C
mL/min	HC[1]	C[2]	C5[3]	C6[4]	Acetic[5]	DH[6]	dimensionless	dimensionless
2.5	0.006	*	0.019	0.019	0.002	*	15.5	0.0
5	0.009	0.009	0.029	0.029	0.0025	0.01	15.0	0.0
10	0.011	*	0.031	0.028	0.021	*	14.8	0.0
15	0.016	*	0.040	0.028	0.030	*	13.5	0.0
20	0.020	*	0.054	0.054	0.070	*	15.0	0.0
R^2	0.98	*	0.98	0.98	0.91	*	0.96	*

TEMPERATURE EFFECT								
T	H(dimensionless)						β_{HC}	β_C
ºC	HC[1]	C[2]	C5[3]	C6[4]	Acetic[5]	DH[6]	dimensionless	dimensionless
185	0.073	000	0.584	0.584	0.20	0.00	15.5	0.0
235	0.400	0.20	0.627	0.627	0.21	0.02	21.0	0.0
285	0.500	0.21	0.650	0.650	0.22	0.23	28.0	4.2
R^2	0.91	-	0.97	0.97	1	-	0.99	-

T	K ($min^{-1} \cdot g^{-1}$)					
ºC	1[a]	2[b]	3[c]	4[d]	5[e]	6[f]
185	0.2	*	0.7081	*	0.0234	0.079
235	1.0	0.0008	1.9821	0.053	0.0238	0.095
285	4.5	0.0220	4.4442	0.248	0.0240	0.120
R^2	0.99	*	0.999	*	0.97	0.98

[1]Hemicellulose. [2]Cellulose. [3] Pentose (Sugar C5). [4]Hexose (Sugar C6). [5]Acetic Acid. [6] Deacetylated hemicellulose.

[a]Hemicellulose breaking in solid phase, [b]Cellulose fractionation in solid phase, [c]Hemicellulose degradation in water, [d]Cellulose degradation in water, [e]Hemicellulose deacetylation, [f]Acetic Acid dissociation, *Parameter not considered due to the low temperature.

Figure 1.

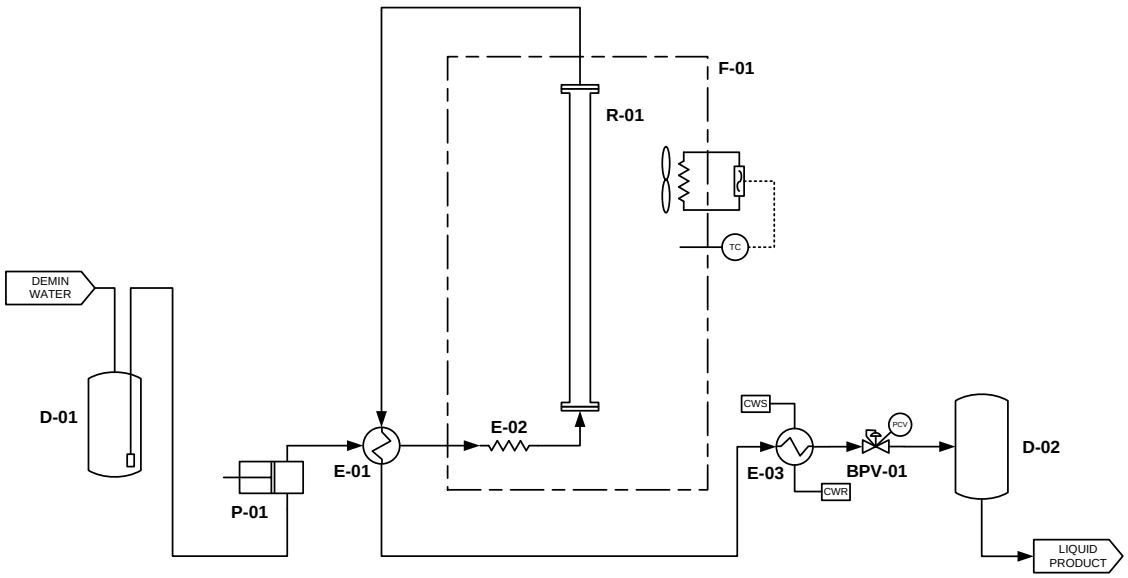
F-01
R-01
TC
DEMIN WATER
D-01
P-01
E-01
E-02
CWS
E-03
CWR
PCV
BPV-01
D-02
LIQUID PRODUCT

Figure 2.

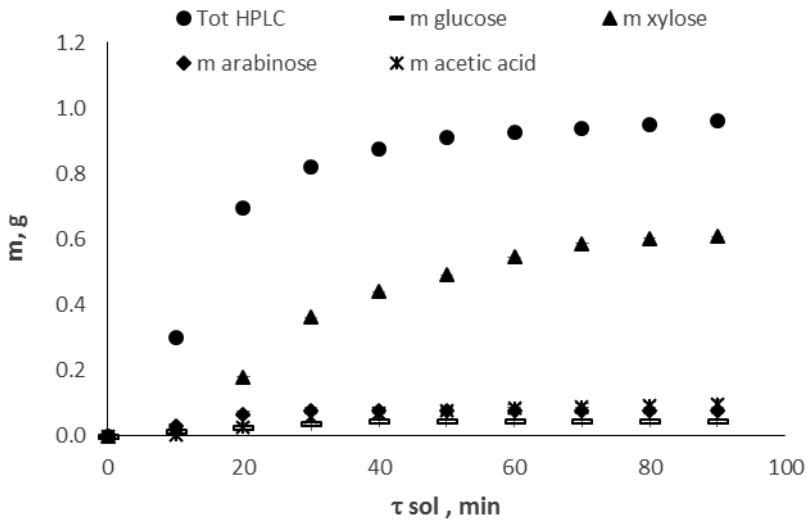
Tot HPLC
m glucose
m xylose
m arabinose
m acetic acid
1.2
1.0
0.8
0.6
0.4
0.2
0.0
m, g
0
20
40
60
80
100
τ sol , min

Figure 3.

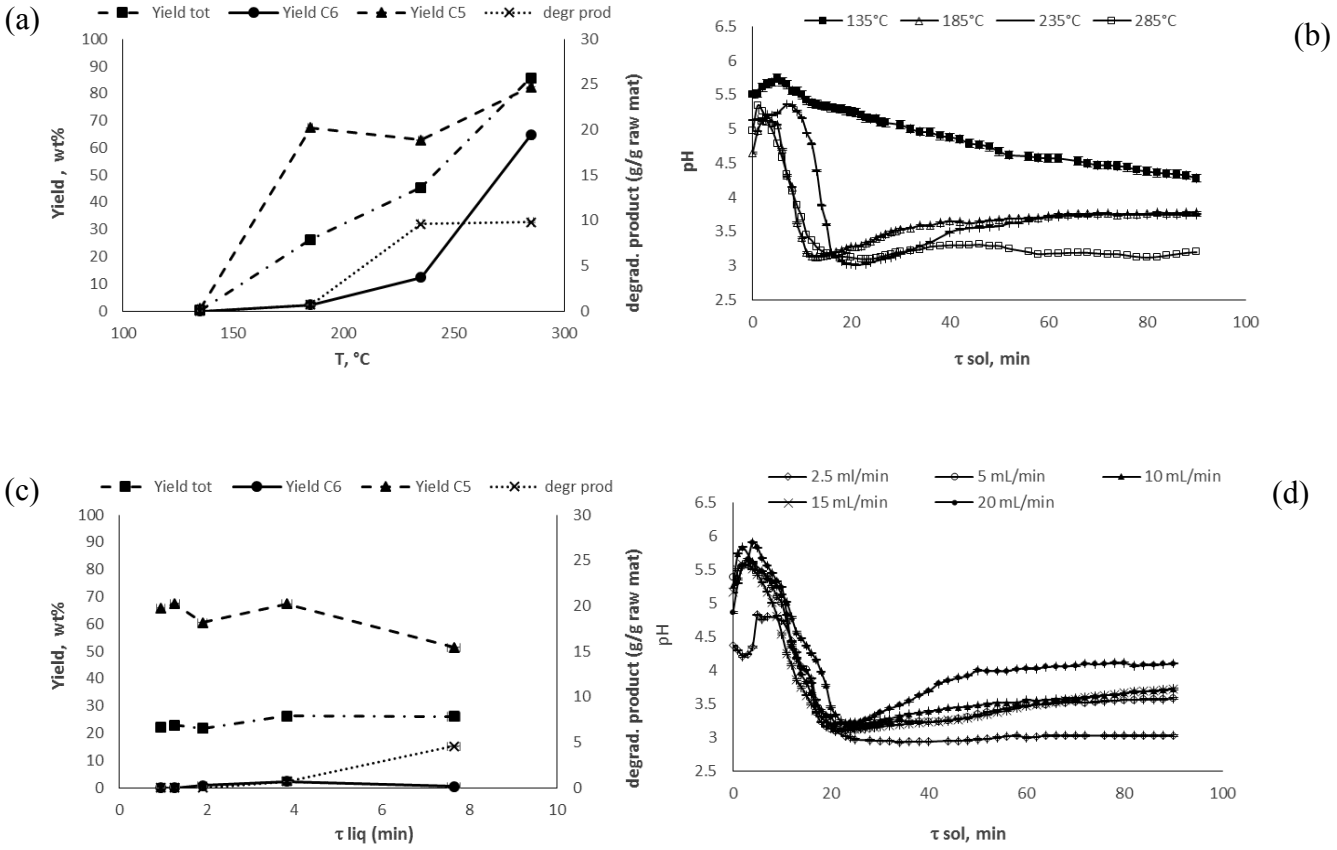
(a)
Yield tot
Yield C6
Yield C5
degr prod
Yield , wt%
degrad. product (g/g raw mat)
T, °C
(b)
135°C
185°C
235°C
285°C
pH
τ sol, min
(c)
Yield tot
Yield C6
Yield C5
degr prod
Yield, wt%
degrad. product (g/g raw mat)
τ liq (min)
(d)
2.5 ml/min
5 mL/min
10 mL/min
15 mL/min
20 mL/min
pH
τ sol, min

Figure 4.

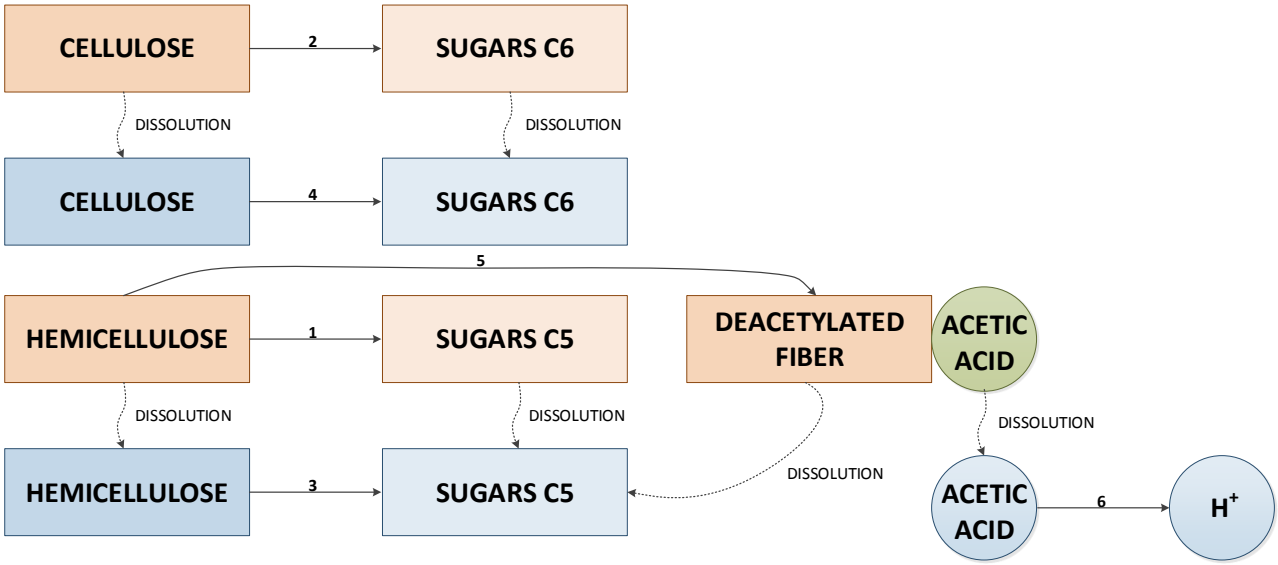
CELLULOSE
2
SUGARS C6
DISSOLUTION
DISSOLUTION
CELLULOSE
4
SUGARS C6
5
HEMICELLULOSE
1
SUGARS C5
DEACETYLATED FIBER
ACETIC ACID
DISSOLUTION
DISSOLUTION
DISSOLUTION
DISSOLUTION
HEMICELLULOSE
3
SUGARS C5
ACETIC ACID
6
H+

Figure 5.

(a)

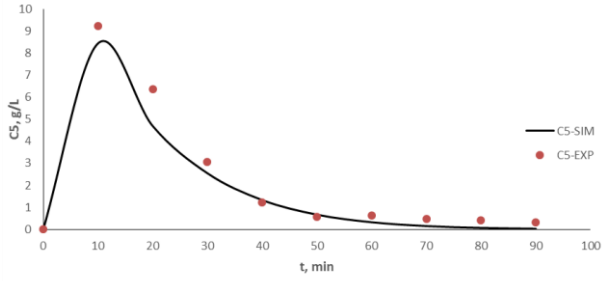

(d)

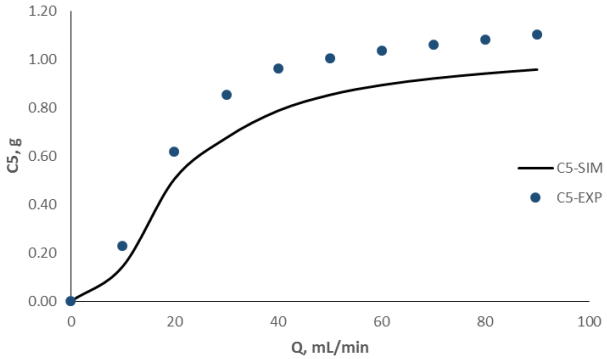

(b)

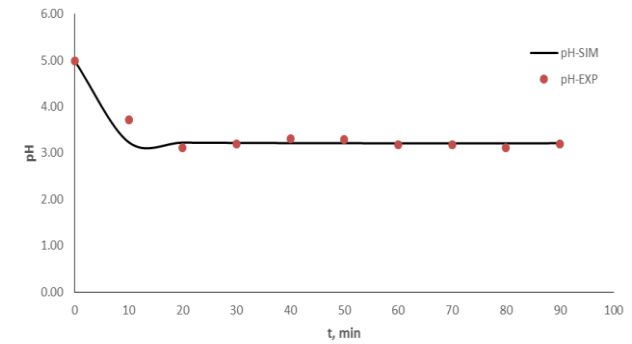

(e)

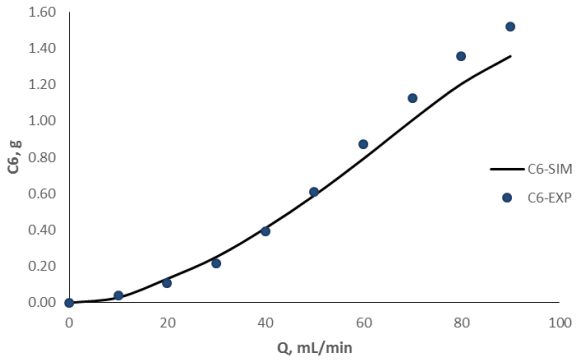

(c)

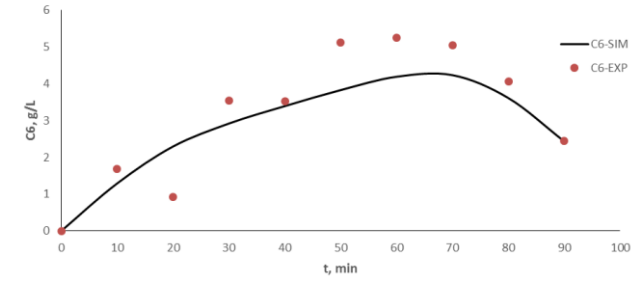

Figure 6.

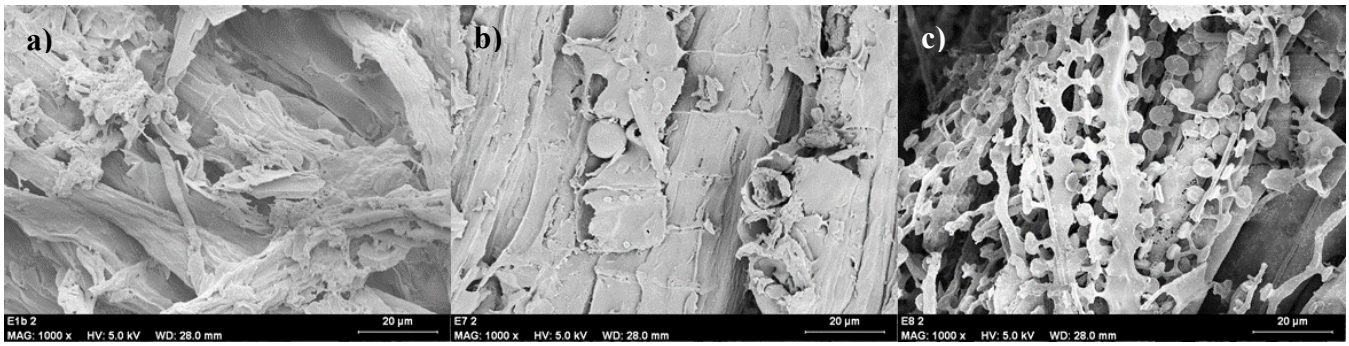
a)
E1b 2
MAG: 1000 x HV: 5.0 kV WD: 28.0 mm
20 µm
b)
E7 2
MAG: 1000 x HV: 5.0 kV WD: 28.0 mm
20 µm
c)
E8 2
MAG: 1000 x HV: 5.0 kV WD: 28.0 mm
20 µm